Available online at www.sciencedirect.com
SCIENCE DIRECT®
Journal of Nuclear Materials 323 (2003) 101–107
journal of nuclear materials
www.elsevier.com/locate/jnucmat

Heat capacity of hydrogenated Zircaloy-2 and high Fe Zircaloy

K. Une *, S. Ishimoto

Global Nuclear Fuel-Japan Co., Ltd., 2163, Narita-cho, Oarai-machi, Higashi Ibaraki-gun, Ibaraki-ken 311-1313, Japan

Received 20 November 2002; accepted 23 August 2003

Abstract

Heat capacities (C_p) of non-hydrogenated and hydrogenated Zircaloy-2 and high Fe Zircaloy were measured in the temperature range from 350 to 873 K, using a differential scanning calorimeter. The hydrogen concentrations in the two types of alloys ranged from 26 to 1004 ppm. The C_p values of the as-received alloys with 26–29 ppm hydrogen were in good agreement with literature data for low hydrogen Zircaloys. From this finding and observation of almost the same enthalpy changes for hydride dissolution for both alloys, it was concluded that there was no difference in C_p values between the two types of hydrogenated Zircaloys. The dissolution enthalpy of hydrides calculated from C_p data was 41.0 kJ/g-atom H. For Zircaloy-2 samples with higher hydrogen concentrations than 700 ppm, the phase transition from $\alpha + \delta$ to $\alpha + \beta$ was observed at the eutectoid temperature of 824–827 K. Two types of models describing an additional heat capacity due to the hydride dissolution were presented based on the present C_p data and previously derived terminal solid solubility of hydrogen.

PACS: 28.41.Bm; 64.75.+g

1. Introduction

Zirconium-based alloys are widely used as fuel cladding and fuel structural materials in light water reactors, because of their good characteristics, including low neutron absorption cross section and corrosion resistance.

In the last decade, maximum fuel discharge burnups have been gradually extended in many countries, in order to reduce the amount of spent fuels and to improve the fuel cycle cost. When extending fuel burnups, corrosion and also hydrogen pickup in Zr alloys gradually increase. In particular, hydrogen behavior plays an important role in embrittlement of Zr alloys. When the hydrogen concentration in Zr alloys exceeds the terminal solid solubility, zirconium hydride is precipitated, which brings about a marked ductility reduction of Zr alloys. In addition to the impact on mechanical properties, the hydrogenation of Zr alloys changes the thermo-physical properties such as heat capacity and thermal conductivity, both of which are very important for the evaluation of fuel temperature under normal, transient and accident reactor conditions. Although there are some data sets of heat capacity for non-hydrogenated Zr [1], Zircaloy-2 [2,3] and Zircaloy-4 [4], the data for samples containing hydrogen up to the level of several hundreds ppm supposed at high burnups are very limited. In the C_p measurements for a Zircaloy-2 specimen with 115 ppm hydrogen [2] and a Zr specimen with 300 ppm hydrogen [5], clear additional heat capacities due to dissolution of hydrides were observed. In MATPRO-V.11 [6], the effect of hydrogen addition on C_p was modeled, based on a concept of hydride dissolution energy and terminal solid solubility of hydrogen. Then the model was verified only using the latter datum.

New Zr alloys for use as BWR fuel claddings and spacer materials at high burnups, have been developed from the viewpoint of improvement of corrosion resistance and hydrogen pickup properties. One promising candidate is high Fe Zircaloy, which has an increased amount of Fe above the upper limit of the Zircaloy-2

* Corresponding author. Tel.: +81-29 267 9011; fax: +81-29 267 9014.
E-mail address: katsumi.une@gnf.com (K. Une).

0022-3115/$ - see front matter © 2003 Elsevier B.V. All rights reserved.
doi:10.1016/j.jnucmat.2003.08.029

chemical specification. In our previous irradiation tests in commercial BWRs and test reactors, it has given better performances than Zircaloy-2 [7]. Therefore, systematic C_p data for this new alloy as well as the currently produced Zircaloy-2, which contain a wide range of hydrogen concentration, are needed.

In the present study, systematic data sets of C_p for the current Zircaloy-2 and improved high Fe Zircaloy for BWRs, which were hydrogenated to a maximum level of 1004 ppm, were derived by differential scanning calorimetry (DSC) in the temperature range from 350 to 873 K. Then two types of models describing an additional heat capacity due to the hydride dissolution were presented based on the present C_p data and previously derived terminal solid solubility of hydrogen [8].

2. Experimental

2.1. Materials

Table 1 shows the chemical composition of Zircaloy-2 and high Fe Zircaloy plates, which were used for the present C_p measurements. The two plates were fabricated by cold rolling and a heat treatment process, in the same way as the current Zircaloy-2 cladding. The final annealing temperature was 848 K, bringing about a recrystallized grain structure. The hydrogen concentration of the as-received materials was 26–29 ppm.

Test samples were hydrided by two methods. One was gaseous hydrogenation at 573 K in an Ar/3%H_2 mixed gas, and absorbed hydrogen concentrations were controlled by varying reaction duration. After hydrogen charging, the samples were homogenized at 673 K for 8 h in pure Ar. The other hydrogen charging was carried out by a corrosion reaction in water vapor of 10.3 MPa at 803 K for reaction durations of 1–6 days. The former method was applied to prepare lower hydrogen content samples (<100 ppm), and the latter method for higher hydrogen content samples (>100 ppm). After hydriding, the surface corrosion layer was removed by grinding. Then the test samples were cut into shapes approximately 4 mm square and 0.5 mm thick, and weighing about 40–50 mg. The hydrogen concentration in all the samples was chemically analyzed by the hot vacuum extraction method with an accuracy of ±3%.

Table 1
Chemical composition (wt%) of Zircaloy-2 and high Fe Zircaloy

Material	Sn	Fe	Cr	Ni	O	Zr
Zry-2	1.37	0.17	0.11	0.07	0.13	Balance
High Fe Zry	1.46	0.26	0.10	0.05	0.15	Balance

2.2. Differential scanning calorimetry

Heat capacities of hydrogenated Zircaloy-2 and high Fe Zircaloy were measured by using a differential scanning calorimeter (DSC: Netzsch DSC-404, high temperature type). The instrument is based on the measurement of thermal response of a sample crucible compared to a reference or blank crucible when the two are heated up uniformly at a constant heating rate. After obtaining a base line of the instrument using two blank crucibles, first and second measuring runs were made using a standard material of sapphire and then a sample. From these three data sets and literature C_p values of sapphire, C_p values of the sample were calculated. Before the DSC measurements, temperature of the instrument was calibrated using melting points of four standard metals (In, Bi, Zn, Al). The C_p measurements were carried out in purified Ar at the flow rate of 50 cm^3/min. In all the measurements, the sample was pre-conditioned at 323 K for 20 min, and heated up to 873 K from 323 K at the heating rate of 10 K/min. After the heat up stage, the sample was cooled down to 393 K at the rate of 10 K/min, and then furnace-cooled. The second run data was adopted on calculating C_p values, so as to diminish the memory of sample fabrication processes.

In order to check the accuracy of the instrument, the heat capacities of α-Al_2O_3 having almost the same shape as the present Zircaloy samples had been previously measured and compared with literature data. Based on this, the accuracy of the instrument used in this study was estimated to be ±4%. The details of the DSC instrument and experimental procedure were described previously [9].

3. Results and discussion

3.1. Heat capacities of hydrogenated Zircaloy-2

The results of heat capacities of as-received Zircaloy-2 sample, containing 26 ppm hydrogen, are shown in Fig. 1, in which literature data of low hydrogen Zircaloy-2 [2,3] and Zircaloy-4 [4] (<10 ppm hydrogen assumed) are also given for a comparison. The present C_p data in the temperature range of 350 to 873 K are in accordance with the literature data within the experimental error of ±4%. Nevertheless, looking carefully at the curves in the low temperature region shows that the data of the present 26 ppm sample appear to slightly rise up around 520 K. This is attributable to a hydride dissolution effect, because the complete dissolution temperature of hydrides for the 26 ppm sample is estimated to be 517 K, based on the previous terminal solid solubility data [8]. These results demonstrate the reliability of the present measuring system of C_p.

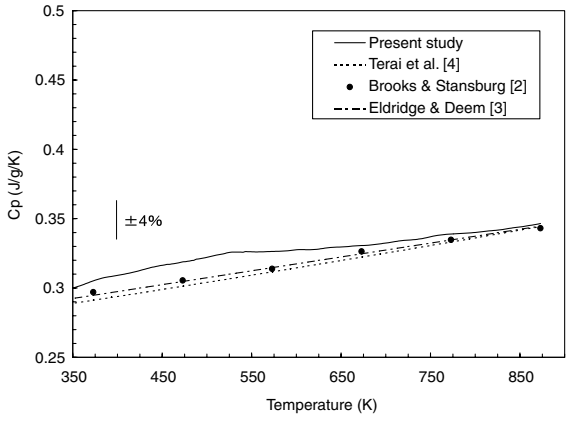

Fig. 1. Heat capacity of as-received Zircaloy-2 with literature values for low hydrogen Zircaloys.

Fig. 2 compares heat capacities of hydrogenated Zircaloy-2 samples with various hydrogen concentrations of 26, 40, 106, 196, 287 and 505 ppm. Among the six C_p curves, the data of 26 ppm are nearly regarded as a base line of Zircaloy-2. In the C_p curves, two types of peaks are seen: (1) small peaks around 460 K, especially noticeable for the high concentration samples of 287 and 505 ppm and (2) broad peaks due to the endothermic reaction, with peak size and peak terminal temperature depending considerably on hydrogen concentration. For the first low temperature peaks, the phase transition from γ hydride (ZrH) to $\alpha + \delta$ hydride (ZrH_x) may be anticipated. There has been evidence [10] that supports the γ- to δ-phase transition around 460 K. From neutron diffraction measurements at high temperatures for Zr–2.5wt%Nb alloy, about 60% of γ-phase, coexisting with δ-phase at lower temperatures, transformed into δ-phase in a temperature range of 453–473 K [10]. On the other hand, γ- to δ-phase transition was detected at the

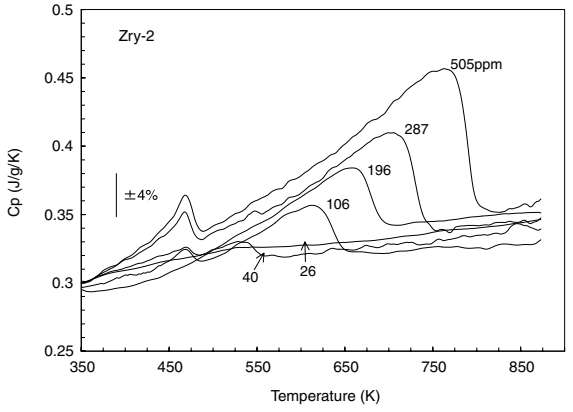

Fig. 2. Heat capacities of hydrogenated Zircaloy-2 with hydrogen concentrations up to 505 ppm.

higher temperature of 528 K for unalloyed Zr from DTA measurements [11]. Moreover, according to C_p data of $ZrD_{1.01}$ (containing three phases α, δ and γ) by a scanning adiabatic calorimeter, a reversible and continuous anomaly was observed between 390 and 620 K, resulting from $\gamma \rightarrow \alpha + \delta$ transformation [12]. γ hydride has been widely accepted to be a metastable phase existing in the region of $\alpha + \delta$ phase; the formation of γ hydrides appears to be favored by high rates of quenching from hydrogen solution state, whereas lower rates favor the formation of the stable δ hydride phase [13]. Then the volume proportion of γ to δ phase is mainly dependent on cooling rate. The boundary of the cooling rate, above which some γ hydrides are formed, has been reported to be about 2 K/min [14]. The cooling rate used in the last heat treatment of the present samples before C_p measurements was 10 K/min. Therefore, the present samples must contain some portion of γ hydrides besides δ hydrides.

The second broad peaks result from the endothermic reaction of the dissolution of δ hydrides. The terminal temperature for a complete hydride dissolution, at which C_p curves rapidly swing back to the base line, significantly depends on hydrogen concentration in the samples. In our previous paper [8], the terminal solid solubility for the dissolution of hydrides (TSSD), which was derived solely from the DSC peak obtained during heatup for the same samples as used in the preset heat capacity measurements, was formulated as

$$C_{\mathrm{TSSD}}(\mathrm{ppm}) = 1.28 \times 10^5 \exp(-36\,540/RT). \quad (1)$$

Here R is the gas constant (8.314 J/(K mol)) and T, the temperature in K. The resulting apparent activation energy for TSSD solvus was 36.5 kJ/mol.

The C_p values of $\alpha + \delta(+\gamma)$ phase at the starting temperature of 350 K and of α phase at the maximum temperature of 873 K for the various samples, appear to coincide with each other within ±4% error. This indicates that hydride precipitation and hydrogen solution in the Zr matrix do not have a large influence on C_p. In fact, an additional heat capacity brought about by the coexistence of δ hydrides of up to 500 ppm in α phase, which was calculated from the summation rule by using C_p data of δ hydrides [15], is much smaller than the experimental error of ±4%.

The C_p curves of Zircaloy-2 samples with higher concentrations of hydrogen above 700 ppm are shown in Fig. 3(a) in normal scale and Fig. 3(b) in large scale. For these samples, in addition to the two types of peaks due to the phase transition of γ–δ and the hydride dissolution, third-type sharp and large peaks are detected at higher temperatures above 820 K. The onset temperature of the large peaks of the 740 and 792 ppm specimens is determined to be 824–827 K, which makes them attributable to the phase transition from $\alpha + \delta$ to $\alpha + \beta$,

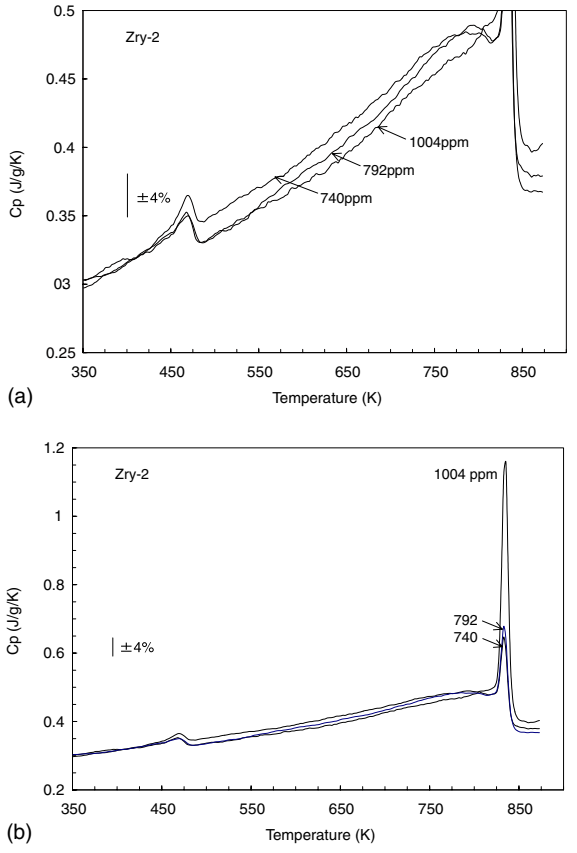

Fig. 3. Heat capacities of hydrogenated Zircaloy-2 with hydrogen concentrations of 740–1004 ppm. (a) normal scale; (b) large scale.

because the measured transition temperatures are in good agreement with literature eutectoid temperatures of 820–823 K [13,16].

3.2. Heat capacities of hydrogenated high Fe Zircaloy

Fig. 4 shows the results of heat capacities of three kinds of hydrogenated high Fe Zircaloy with 91, 137 and 410 ppm hydrogen, in addition to the as-received material with 29 ppm hydrogen.

When comparing C_p values of the as-received high Fe Zircaloy with the data of the as-received Zircaloy-2, they are in good accordance with each other, the difference between them being less than 3%. It is concluded that there is no difference in C_p between Zircaloy-2 and high Fe Zircaloy. This result may be reasonably accepted, because of almost the same C_p values for Zircaloy-4 and Zircaloy-2 [2–4] as shown in Fig. 1, and a minor difference in Fe content between the present Zircaloy-2 and high Fe Zircaloy as given in Table 1.

The same two types of peaks are seen as observed for Zircaloy-2 in Fig. 2; (1) the small peaks around 460 K,

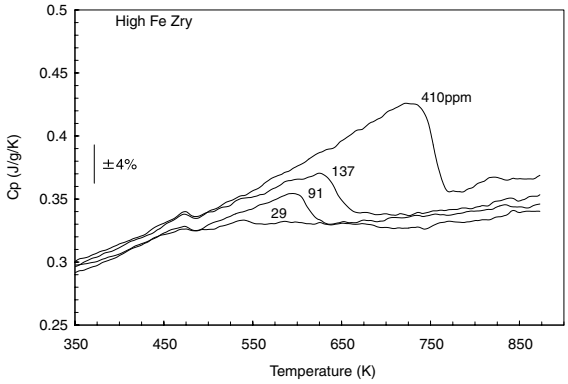

Fig. 4. Heat capacities of as-received and hydrogenated high Fe Zircaloy with hydrogen concentrations of 29–410 ppm.

probably due to the phase transition of γ to $\alpha + \delta$ hydride, and (2) the broad peaks due to the hydride dissolution. In our previous paper [8], a unified equation of the terminal solid solubility of hydrogen for dissolution of hydrides (Eq. (1)) was derived for both alloys. From this result and the dissolution enthalpy changes of hydrides (see next section), it is concluded that there is no difference in C_p between the two hydrogenated types of alloys. Nevertheless, the magnitude of the first C_p peaks around 460 K for high Fe Zircaloy appears to be smaller than that for Zircaloy-2 in Fig. 2. Though the reason for this cannot be assigned, more amounts of the small precipitates of Zr–Fe–Ni and Zr–Fe–Cr in high Fe Zircaloy may affect this phenomenon.

3.3. Enthalpy changes of hydride dissolution

The areas of hydride dissolution peaks for the hydrogenated alloys beyond anticipated base lines of C_p correspond to the enthalpy changes of hydride dissolution (ΔH_{H}). When drawing the base lines, a linear interpolation was made between two C_p data at 373 K and the terminal temperatures of hydride dissolution peaks. The derived ΔH_{H} values per g-atom hydrogen are plotted against hydrogen concentration in Fig. 5.

Though a scatter in ΔH_{H} exists between Zircaloy-2 and high Fe Zircaloy in the low hydrogen concentration range of less than 200 ppm, it is clarified that ΔH_{H} is roughly independent of hydrogen concentration. The average ΔH_{H} is 41.0 ± 1.4 kJ/g-atom H. This value is about 4.5 kJ/g-atom H larger than the apparent activation energy of 36.5 kJ/g-atom H, which was derived from the TSSD solvus of Eq. (1). Somewhat larger enthalpies obtained from C_p curves may be attributed to an additional enthalpy change due to the phase transition from γ to $\alpha + \delta$ hydride. The small peaks, due to the phase transition, are detected around 460 K in Figs. 2–4. Moreover, assuming γ hydride can coexist in $\alpha + \delta$ as a metastable phase [10,12,13,16], a continuous phase

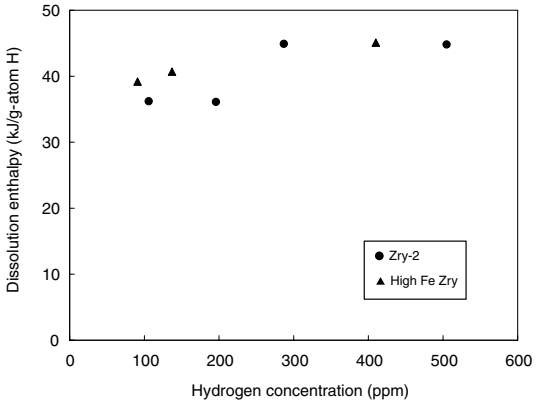

Fig. 5. Enthalpy changes of hydride dissolution for hydrogenated Zircaloys.

transformation may contribute to additional enthalpy change in a wider temperature range. Reported ΔH_H values, which were evaluated from C_p data, are 38.6 kJ/g-atom H for a 115 ppm Zircaloy-2 specimen [2] and 46.0 kJ/g-atom H for a 300 ppm Zr specimen [5].

3.4. Heat capacity model for hydrogenated Zircaloys

By using the TSSD solvus of Eq. (1) reported in our previous paper [8] and the enthalpy change of hydride dissolution obtained in this study, an additional heat capacity (ΔC_p) due to the hydride dissolution was modeled, following the same procedure as the model of MATPRO-V.11 [6]. In the MATPRO model, the ΔC_p is expressed as in a form of

$$\Delta C_p = A/T^2 \exp(-E/T)[\exp((T - T_{TSSD})/\phi T_{TSSD}) + 1]^{-1}, \quad (2)$$

where E is the constant of 4955 K which was calculated from the enthalpy change ($\Delta H_H = 41.0$ kJ/g-atom H) of hydride dissolution, T_{TSSD}, the dissolution temperature of hydrides in K given by Eq. (1), and A and ϕ, the fitting parameters. The first term ($A/T^2 \exp(-E/T)$) of Eq. (2) is obtained by differentiating the energy to dissolve hydride in a type of equation of the form $\propto \exp(-\Delta H_H/RT)$. The second term ($[\exp((T - T_{TSSD})/\phi T_{TSSD}) + 1]^{-1}$) of Eq. (2) is an empirical factor to express the fact that the C_p data do not show an instant termination of hydride solution with increasing temperature. The best fitted parameters of A and ϕ become 4.5×10^7 J K/g and 0.01, when paying attention simultaneously to the measured dissolution temperature of T_{TSSD} and the measured maximum C_p value.

In addition to the modified MATPRO model, we presented another empirical model by fitting the additional heat capacity (ΔC_p) above 350 K on the assumption that ΔC_p increases linearly with temperature, which is expressed by

$$\Delta C_p = B(T - 350)[\exp((T - T_{TSSD})/\phi T_{TSSD}) + 1]^{-1} \quad \text{for } T > 350 \text{ K}, \quad (3)$$

$$B = 1.152 \times 10^{-4} + 3.216 \times 10^{-7} C_H,$$

where C_H is the hydrogen concentration in ppm and the second term of Eq. (3) is the same as in Eq. (2). Naturally, Eq. (3) is only valid in the range of $91 \leqslant C_H \leqslant 506$ ppm.

Figs. 6 and 7 compare the measured and calculated C_p values for the hydrogenated Zircaloy-2 and high Fe Zircaloy, respectively. Two examples are made for the two types of alloys containing hydrogen levels of about 100 and 400–500 ppm. In the calculation, the C_p equation (Eq. (4)) for Zircaloy-2 proposed by Eldridge and Deem [3] was adopted as the base line of C_p for non-hydrogenated Zircaloys.

$$C_p = 0.2847 + 9.988 \times 10^{-5}(T - 273). \quad (4)$$

For all the cases, the modified MATPRO model of Eq. (2) underestimates the ΔC_p compared to the measured

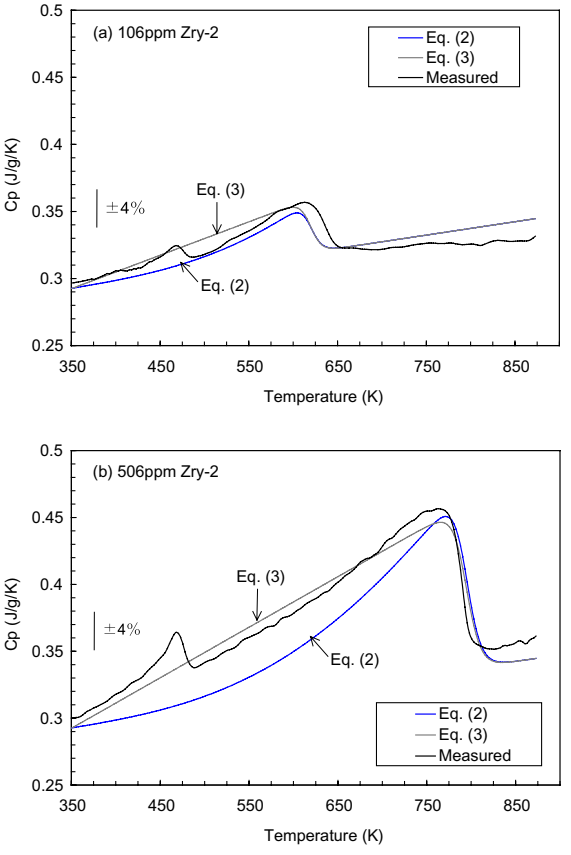

Fig. 6. Comparison between measured and calculated heat capacities for hydrogenated Zircaloy-2. (a) 106 ppm; (b) 506 ppm.

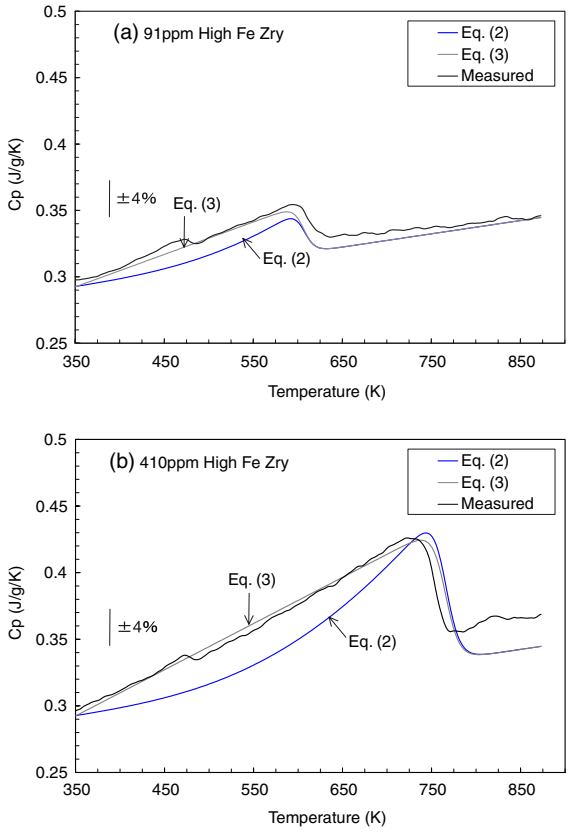

Fig. 7. Comparison between measured and calculated heat capacities for hydrogenated high Fe Zircaloy. (a) 91 ppm; (b) 410 ppm.

data, and this tendency tends to become more intense with increasing hydrogen concentration. This difference may be attributed to a continuous phase transformation from metastable γ hydride to α + δ hydride [12], whose contribution is not taken into consideration in Eq. (2). Nevertheless, for the lower hydrogen samples of about 90–110 ppm (Figs. 6(a) and 7(a)), a good agreement is seen between the measured C_p values and the calculated ones by the two models within the error of ±2.5%. For the higher hydrogen samples of about 400–500 ppm (Figs. 6(b) and 7(b)), the modified MATPRO model of Eq. (2) gives lower C_p by at most 6–7% than the measured data, while the empirical model of Eq. (3) presents a good prediction up to the dissolution temperatures of hydrides.

4. Conclusions

Heat capacities (C_p) of non-hydrogenated and hydrogenated Zircaloy-2 and high Fe Zircaloy were measured in the temperature range of 350 to 873 K, using a differential scanning calorimeter. The hydrogen concentrations in the two types of alloys ranged from 26 to 1004 ppm.

The C_p values of the as-received Zircaloy-2 and high Fe Zircaloy with 26–29 ppm hydrogen were in agreement with literature data for low hydrogen Zircaloys within the accuracy of the apparatus of ±4%. From this result and almost the same enthalpy changes for hydride dissolution for both alloys, it was concluded that there was no difference in C_p values between the two types of hydrogenated Zircaloys. The dissolution enthalpy of hydrides calculated from C_p data was 41.0 kJ/g-atom H for both the materials. A small C_p peak, which probably resulted from the phase transition from γ hydride (ZrH) to α + δ hydride (ZrH_x), was observed around 460 K. For Zircaloy-2 samples with higher hydrogen concentrations above 700 ppm, the phase transition from α + δ to α + β was observed at the eutectoid temperature of 824–827 K.

The additional heat capacity (ΔC_p) due to the hydride dissolution was modeled by two types of formulations, and they were verified using the present C_p data of the hydrogen range of 91–506 ppm. One was a modified MATPRO C_p model, in which the terminal solid solubility data obtained in our previous study and the enthalpy change of hydride dissolution obtained in this study were utilized. The other was a simple empirical model. They were expressed by the equations

$$\Delta C_p = A/T^2 \exp(-E/T)[\exp((T - T_{\mathrm{TSSD}})/\phi T_{\mathrm{TSSD}}) + 1]^{-1} \quad \text{(modified MATPRO model)},$$

$$\Delta C_p = B(T - 350)[\exp((T - T_{\mathrm{TSSD}})/\phi T_{\mathrm{TSSD}}) + 1]^{-1} \quad \text{for } T > 350 \text{ K} \quad \text{(empirical model)},$$

$$B = 1.152 \times 10^{-4} + 3.216 \times 10^{-7} C_{\mathrm{H}},$$

where E is the constant derived from the enthalpy change of hydride dissolution, T_{TSSD}, the dissolution temperature of hydrides, and C_{H}, the hydrogen concentration in ppm. The recommended values were $E = 4955$ K, $A = 4.5 \times 10^7$ J K/g and $\phi = 0.01$. The calculated C_p values by the two models were in good agreement with the measured data within the error of ±2.5% for the Zircaloy samples with lower hydrogen concentrations of about 90–110 ppm. However, for the higher hydrogen samples of about 400–500 ppm, the modified MATPRO model gave lower C_p by at most 6–7% than the measured data, while the empirical model presented a good prediction.

References

[1] A.F. Guillermet, High Temperatures-High Pressures 19 (1987) 119.

[2] C.R. Brooks, E.E. Stansburg, J. Nucl. Mater. 18 (1966) 233.
[3] E.A. Eldridge, H.W. Deem, BMI-1803, 1967.
[4] T. Terai, Y. Takahashi, S. Masumura, T. Yoneoka, J. Nucl. Mater. 247 (1997) 222.
[5] J. Scott, PhD thesis, University of Tennessee, 1957. The results are reproduced in Ref. [6].
[6] D.L. Hagrman, G.A. Reymann, (Eds.), MATPRO-V11, TREE-NUREG-CR-0497, 1979.
[7] S. Ishimoto, T. Kubo, R.B. Adamson, Y. Etoh, K. Ito, Y. Suzawa, in: Proc. Int. Topical Mtg. on LWR Fuel Performance, Park City, 10–13 April 2000, p. 499.
[8] K. Une, S. Ishimoto, J. Nucl. Mater., in press.
[9] M. Amaya, K. Une, K. Minato, J. Nucl. Mater. 294 (2001) 1.
[10] J.H. Root, R.W.L. Fong, J. Nucl. Mater. 232 (1996) 75.
[11] S.M. Mishra, K.S. Sivaramakrishnan, M.K. Asundi, J. Nucl. Mater. 45 (1972) 235.
[12] I.O. Bashkin, V.Yu. Malyshev, M.M. Myshlyaev, Sov. Phys. Solid State 37 (1992) 1182.
[13] F. Zuzek, J.P. Abriata, Bull. Alloy Phase Diagrams 11 (1990) 385.
[14] B. Nath, G.W. Lorimer, N. Ridley, J. Nucl. Mater. 58 (1975) 153.
[15] S. Yamanaka, K. Yamada, K. Kurosaki, M. Uno, K. Takeda, H. Anada, T. Matsuda, S. Kobayashi, J. Nucl. Mater 294 (2001) 94.
[16] A. Aladjem, in: F.A. Lewis, A. Aladjem (Eds.), Zirconium–Hydrogen (Chapter 7) in Hydrogen Metal System I, Balaban, 1996.